Research Article

APPLICATION OF SUPPORTED COLLOIDAL GOLD NANOPARTICLES IN THE OXIDATION OF BENZYL ALCOHOL

AHMAD ALSHAMMARI,[1*] ANGELA KÖCKRITZ,[2] V. NARAYANA KALEVARU,[2] ABDULAZIZ BAGABAS,[1] ABDULAZIZ ALROMAEH,[1] ANDREAS MARTIN[2]

[1] Materials Science Research Institute (MSRI), King Abdulaziz City for Science and Technology (KACST), P. O. Box 6086, Riyadh 11442, Saudi Arabia
[2] Department of Heterogeneous Catalytic Processes, Leibniz Institute for Catalysis, Albert-Einstein-Str. 29a, 18059 Rostock, Germany

Corresponding Author: aalshammari@kacst.edu.sa

Abstract

Preparation and understanding the formation of unsupported and supported colloidal gold nanoparticles (AuNPs) have considerable importance in nanocatalysis due to their beneficial properties. In the present study, colloidal AuNPs were prepared in aqueous solution by one-step chemical reduction of tetrachloroauric acid ($HAuCl_4$) using six different reducing agents, namely: citric acid, sodium citrate, iso-ascorbic acid, sodium borohydride, tannic acid and sodium thiocyanate.. The combination of two reductants (sodium citrate + tannic acid) –was shown to have a remarkable change in the size and stability of colloidal AuNPs. Hence, Colloidal AuNPs were impregnated onto a suitable oxidic supports such as CaO, TiO_2, and Al_2O_3. Unsupported and supported colloidal AuNPs were characterized by UV-vis, XRF, ICP, BET, XRD, and TEM. In addition, the oxidation of benzyl alcohol to benzaldehyde with oxygen using colloidal AuNPs supported on CaO, TiO_2, Al_2O_3 was investigated. Among all, colloidal AuNPs supported on TiO_2 showed the best catalytic activity due to the smaller size of AuNPs formed in this catalyst.

Keywords: colloidal gold nanoparticles, supported gold, particle size, combination of reductant, oxidation of alcohol

Introduction

Colloidal gold nanoparticles (AuNPs) have continued to attract increasing attention due to their amazing properties and potential applications in different areas such as catalysis (Alshammari et. al., 2012; Hashmi and Hutchings, 2013; Prasad and Stoeva, 2003; Jaramillo, et al., 2003; Mohr, et al., 2003; Haruta, 2005,2002), chemical sensors (Cheng and Chau, 2003), (Lee and Asher, 2000), biomedicine, (Goodman et al., 2004; Tiwari et al., 2011), drug delivery (Paciotti et al., 2007) and so on. Particularly in the field of nanocatalysis, a substantial number of studies has been published on the catalytic use of both colloidal gold nanoparticles and supported AuNPs on various carriers (Alshammari et al., 2012; Bond and Thompson, 1999; Hashmi and Hutchings, 2006; Berndt, et al., 2004). It is well known that the catalytic activity of AuNPs strongly depends on

their formation conditions, particle size and size distribution, and also often on interaction with carrier properties (Haruta and Date 2001; Bamwenda et al., 1997). It was reported that when the particle size of Au fell below the range of about 10 nm, they were active catalysts for many reactions ranging from selective oxidation to hydrogenation and hydrochlorination (Haruta, 1997).

In general, metal nanoparticles can be obtained by two distinct routes, which physical method (by subdivision of bulk metals) and chemical method (by the growth of particles staring from metal atoms) (Wang and Xia 2004), (Gaffet et al., 1996). During the past few decades, numerous synthetic methods are reported to manufacture such colloidal AuNPs, however, most of

them used thermal reduction of metal ionic salts and work either in aqueous solutions or in two-phase aqueous/organic systems, with the addition of reducing agents and/or stabilizers ((Turkevich, et al. 1995; Mühlpfordt, 1982). For example, Brust et al. (1994) first reported the two-phase reduction of tetrachloroauric by $NaBH_4$ in the presence of thiols as stabilizer. In addition, some other methods such as electrochemical (Bonet, et al., 1995), sonochemical (Okitsu et al., 2001) and laser pulse (Mafune, et al., 2003) methods have also been used to synthesize AuNPs.

Although, the size of AuNPs depends on various factors such as the nature of reducing agent, the ratio of gold precursor to reducing agent, the initial concentration of gold precursor solution, temperature of reduction or method of preparation. There are still many shortcomings, and systematic studies are also missing in the literature exploring the effects of all these factors on the size of AuNPs (Premkumar et al., 2007). Therefore, there is a need to investigate and understand the influence of such key factors on the size, distribution, morphology and stability of AuNPs under varying conditions as well as with varying reducing agents.

With this background, the present study is aimed to describe the preparation of colloidal AuNPs by chemical reduction of chloroauric acid ($HAuCl_4$) in aqueous solution using six different reductants such as citric acid (CA), sodium citrate (SC), iso-ascorbic acid (IA), sodium borohydride (SB), tannic acid (TA), sodium thiocyanate (ST). Another objective of this study is to support the resulting colloidal AuNPs and testing their catalytic performance towards oxidation of benzyl alcohol (BA) to benzaldehyde (BAl) as a model reaction.

Materials and Methods

Preparation of unsupported colloidal AuNP:

A one-step chemical reduction of tetrachloroauric acid ($HAuCl_4$) solution was carried out using different reductants. In a typical experiment, 30 ml of a 1.0 mM $HAuCl_4$ solution was heated at 60 °C in a 50 ml beaker. In a second beaker, 8 ml of a 15 mM citric acid (CA) solution was heated to 60 °C. After that, the solution of CA was added quickly to the $HAuCl_4$ solution under stirring (1000 rpm) until the formation of colloidal AuNPs was indicated by color. In addition, the same procedure was carried out using the other reductants such as sodium citrate (SC), iso-ascorbic acid (IA), sodium borohydride (SB), tannic acid (TA), sodium thiocyanate (ST). In addition the combination of TA+SC and ST+SC were also used in a similar procedure to reduce $HAuCl_4$ solution.

Preparation of supported colloidal AuNPs

Preparation of supported AuNPs was obtained in two steps. First step deals with the preparation of colloidal AuNPs as shown previously in section 2.1. In the second step, the above-prepared colloidal AuNPs was impregnated onto a suitable oxidic support (e.g. TiO_2) to obtain slurry, which was stirred for 2 h at room temperature and then the excess solvent was removed by rotary evaporation. The obtained solid was oven dried at 120 °C for 16 h and then calcined at 350 °C for 5 h in air. The loading of gold was fixed at 1wt.%. More details on the synthesis conditions and preparation method are described elsewhere (Alshammari et. al., 2012).

Characterization

UV-vis absorbance spectra of colloidal solutions were acquired with a UV-vis spectrometer (Avantes-2048, light source combined deuterium-halogen). The spectra were collected over a range of 200-1100 nm (with an optical path length of 0.4 cm) as a function of reaction time by directly dipping the optical probe in the reaction vessel under constant stirring. Size, size distribution and zeta potential of colloidal AuNPs were determined at room temperature using dynamic light scattering (DLS, Malvern Instruments Zetasizer (ZS ZEN 4003). Samples were assayed at defined times from the reaction and transferred to cuvette for size and size distribution analysis. Inductively coupled plasma (ICP) results of catalysts were obtained by instrument (model: optima 3000XL) PERKIN ELMER USA, using a microwave pressure digestion (MDS 200; CEM) with hydrofluoric and aqua regia. X-ray fluorescence (XRF) analysis of the catalysts was made using Philips PW 1480 X-ray spectrometer. Catalyst samples (50 mg) were pelletted using a die and taken in the cell of XRF instrument for further determination. The BET surface areas and pore size distribution of the catalysts were obtained on Micrometric Gemini III-2375 (U.S.A) instrument by N_2 physisorption at 77 K. Prior to the measurements, the known amount of the catalyst was evacuated for 2 h at 150 °C to remove physically adsorbed water. The X-ray diffraction (XRD) patterns of the catalysts were recorded on a STADI P (STOE) setup with transmission geometry and equipped with a Ge primary monochromator with $CuK\alpha$ radiation in the 2θ ranges from 5-60° and a position-sensitive detector. TEM analysis was carried out using JEM-2100F high-resolution electron microscopy at a voltage of 200 kV. Sample preparation of unsupported gold particles for TEM is quite simple, involving the depositing of such materials on a carbon coated micro grid. However, supported AuNPs samples were dispersed in water/methanol and treated with ultrasound for 5 min, and then deposited on a carbon grid.

Catalytic tests.

The catalytic tests towards the oxidation of benzyl alcohol (BA) were carried out in a Parr autoclave (Vol. 100 mL). The reaction vessel was charged with 0.15 g of gold colloid catalyst and BA (0.29 mol). The autoclave was flushed three times with O_2 before setting the initial reaction pressure of O_2 at 5 bar. Concerning the start-up procedure, this was performed with the O_2 line opened, and as the O_2 was consumed, it will be automatically refilled from the cylinder, in order to maintain the overall pressure constant. The reaction mixture was stirred (1500 rpm) at 140 °C for 4 h. At the end of the reaction, the solid catalyst was separated by centrifugation. The identification and analysis of the products was made by gas chromatograph (HP 6890 GC), equipped with an ultra-1 column (methyl siloxane) and a flame ionization detector (FID). Samples were collected at the end of the reaction; 600 µL of product sample was added to 400 µL of internal standard (ethylene glycol dibutyl ether) and 1 µL of this mixture was analyzed by GC.

Results and Discussion

Influence of the nature of the reductant on the size and morphology of AuNPs:

UV-vis absorption spectra (Figure 1) of colloidal AuNPs obtained by different reductants showed different surface plasmon (SP) bands, which differ in their λ_{max} and SP band intensities, indicating a clear influence of the reductants on particle size and SP band position of colloidal AuNPs. The spectra were recorded when both the color and absorption intensity of the colloidal samples stayed constant. Among six different reducing agents used, application of IA and TA showed a plasmon band positions with a lower wavelength (520 and 522 nm, respectively) compared to others. These bands were also observed to be somewhat broad and less intense. However, AuNPs prepared by other reducing agents such as SC, SB, CT and CA showed comparable band position (528±1 nm) with some deviations in their band intensities. Interestingly, in case of ST as reductant, UV-Vis results confirmed that the SP resonance becomes weaken and shifts towards higher energy and even disappears sometimes, which indicates that the particle size of AuNPs decreased to 4 nm (Alvarez, et al., 1997). Such phenomenon might be due to the fact that the electrons of small AuNPs exist in discrete energy levels, and gold in bulk state has a continuous absorbance in the UV/vis/IR regions, which is then collapses into a single SP band. Moreover, the nature of the reducing agent has also shown a significant influence on the rate of reduction of the $HAuCl_4$ solution. This means the formation of AuNPs by reduction of Au^{+3} to Au^0 species took varying reaction times ranging from a few seconds to several minutes.

For instance, the use of strong reducing agents such as IA, SB and TA revealed a complete reduction in some seconds (ranging from 3 to 8 sec), while the use of mild reductants such as SC and ST did not show complete reduction until 50 min and 15 min, respectively. In addition, the colloidal AuNPs formed using IA, SB and SB were relatively less stable compared to other reductants.

Average size distribution of colloidal AuNPs produced using different reducing agents was also recorded by DLS. Particle sizes determined by this technique are presented in Figure 2a-f, however, these results do not match with those determined from TEM images. The reduction using ST (f) produced the smallest Au particles with an average particle size of approximately 8 nm while the biggest particles were obtained by use of CA (a) with average size of 49 nm. Reduction using strong reducing agent such as SB (d), IA (c) and TA (e) produced particles with sizes of about 17, 42, 30 nm, respectively, with varying shapes of nanowires and spherical particles. The average particle size obtained with varying reductants changes in the following order: CA > IA > TA > SB > SC > ST. However, the stability of such AuNPs was found to be somewhat different and follows the order: CA and SC (most stable) > SB > IA > ST > TA (not stable).

TEM images of colloidal AuNPs synthesized under similar conditions (1.0 mM of $HAuCl_4$ and 15 mM of reducing agent) using various reductants are shown in Figure 3. CA as reducing agent led to predominantly different shapes of AuNPs with an average particle size of 45 nm; (Fig. 3a), but most of the particles exhibited other structures such as hexagonal shapes. Applying SEM (not shown) particle sizes of about 47 nm were measured for the same sample. This means SEM measurement also gave similar tendency and comparable results with that of TEM, which is an indicative of reliability and supporting evidence on the size of AuNPs in this sample. On the other hand, polyhedral AuNPs with an average particle size of 3±1 nm and 12 nm were obtained using ST and SC, respectively, as shown in Fig. 3f and 3b. In addition, strong reductants, such as IA and SB, have a noticeable influence on the morphology of the colloidal AuNPs (Fig. 3c and d). Most AuNPs produced using IA were spherical, tiny particles with an average diameter size of 38 nm, whereas SB produced wire-like networks with diameters of about 11 nm. Application of TA as reducing agent gave more or less spherical AuNPs with the size of around 25 nm (Fig. 3e).
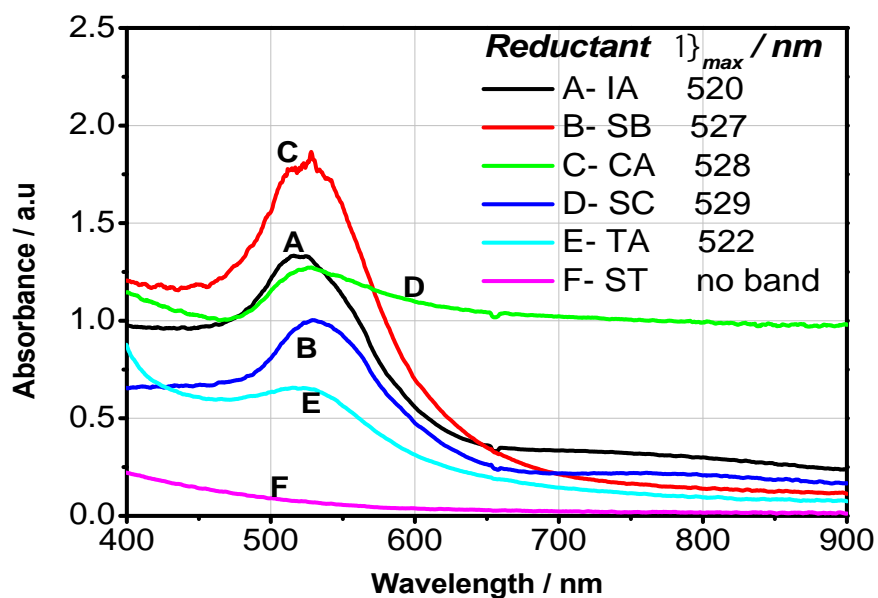
Fig. 1 UV-vis spectra of colloidal nano-gold particles prepared by reduction of 1.0 mM HAuCl$_4$ solution using different reducing agents (IA, SB, CA, SC, TA and ST).
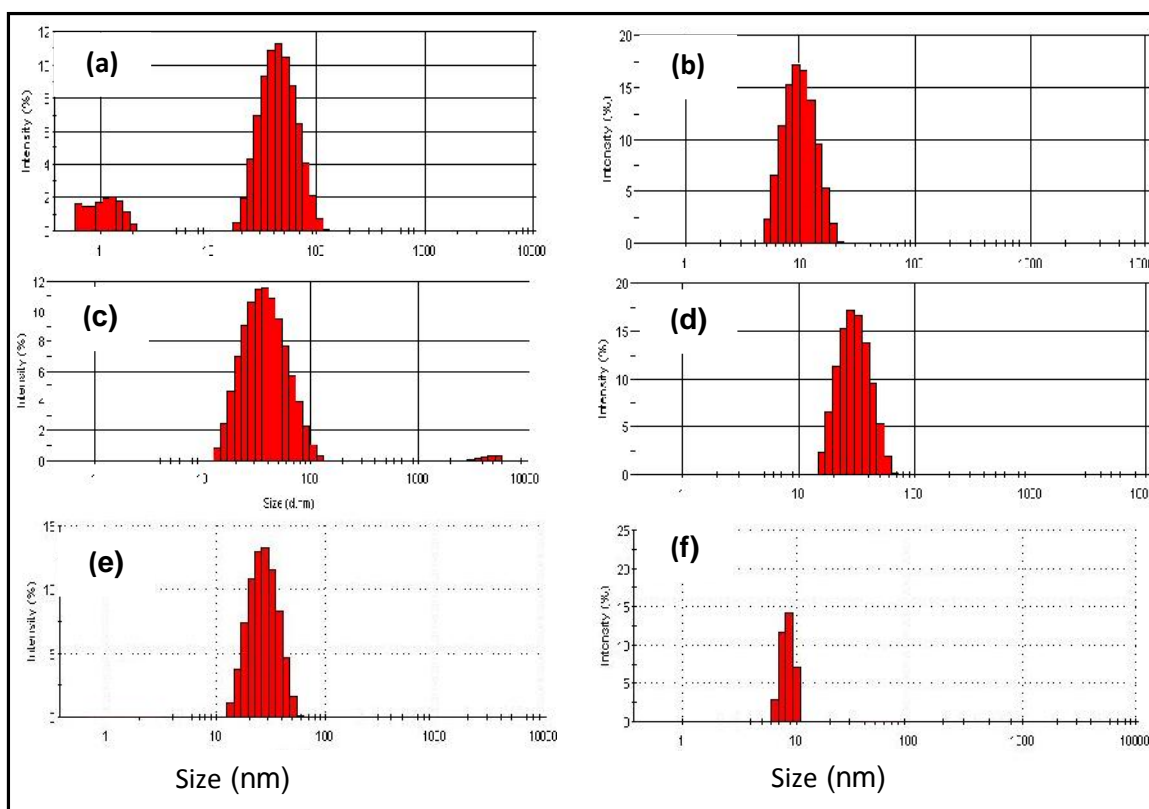

Fig. 2 DLS size distribution of colloidal AuNPs prepared by the reduction of 1.0 mM HAuCl$_4$ using different reducing agents (a- CA, b- SC, c- IA, d- SB, e- TA, f-ST).
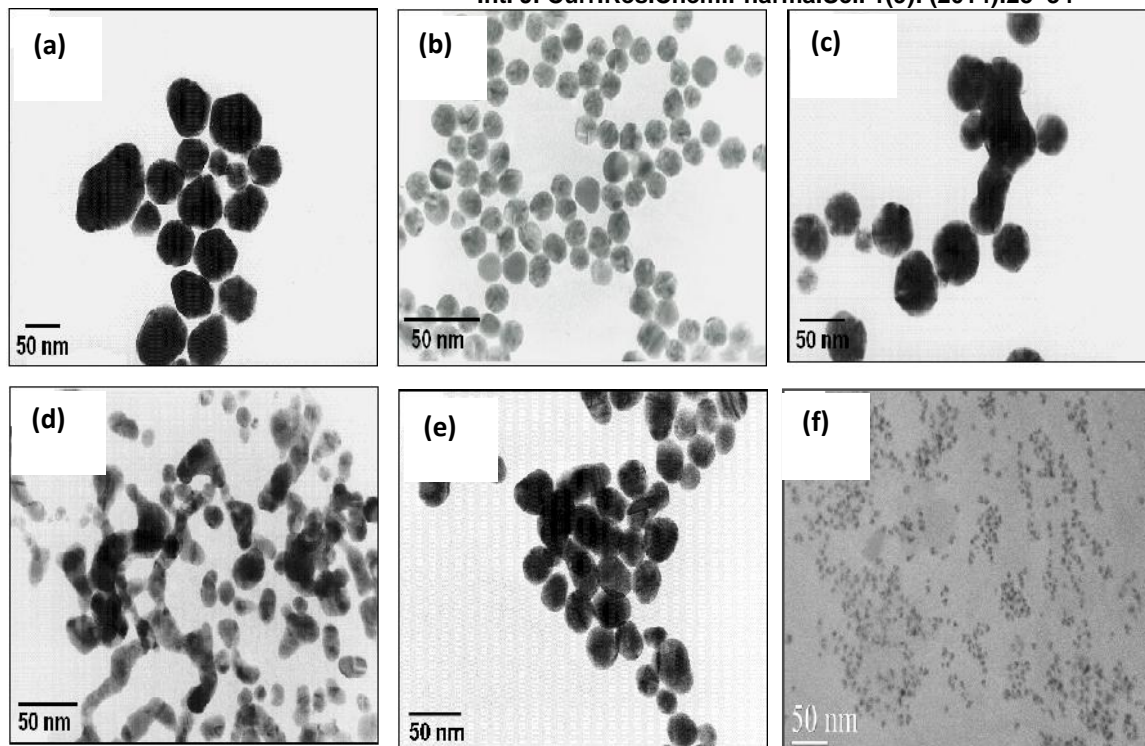
Fig. Representative TEM images of colloidal AuNPs particles prepared by reduction of $HAuCl_4$ solution using different reductant: **(a)** CA, **(b)** SC, **(c)** IA, **(d)** SB, **(e)** TA, **(f)** ST.

Effect of the combination of reductants on the size, shape and stability of colloidal AuNPs.

In order to synthesize relatively stable and small Au nanoparticles with average particle size less than 5 nm, we tried to develop a method to achieve this goal avoiding some common stabilizers such as block copolymers, dendrimers, polymers, etc. It is known that the usage of stabilizers to cap the nanoparticles against agglomeration can affect activity of the nanoparticles (Li and El-Sayed, 2001). Therefore, it is important to maintain the stability of the colloidal AuNPs by the electrostatic or charge stabilization method (Lee, et al., 2005). Herein, a detailed examination on the influence of the combination of two reducing agents on the size, shape and stability of colloidal AuNPs is conducted. These studies were achieved by the addition of a desired amount of SC to a solution of tannic acid and sodium thiocyanate, individually. In the first case, the reduction of gold ions was obtained by the addition of a combination of TA and SC to the $HAuCl_4$ solution. As shown above, TA alone gave AuNPs with average size of 25 nm (Figure 3e) and the colloidal mixture was somewhat unstable, and was also proved optically by the presence of precipitation trace (agglomeration) after the preparation. We have also obtained spectroscopic evidence via zeta potential measurements where the particles have a very low zeta potential value (= 17.4 mV) indicating instability of such particles (http://www.malvern.com/LabEng/industry/colloids/ colloids_stability.html). Surprisingly, the combination of SC and TA significantly affected the particle size where the average size dropped from 25 nm to less than 5 nm (Fig. 4a). In addition, the zeta potential result showed that the colloidal AuNPs were negatively charged with a value of -32.4 mV in the presence of SC while with TA alone the zeta potential was 17.4 mV. The high zeta value could be due to the presence of a large amount of SC ions around the gold nanoparticles, which further stabilizes the particles. In the second case, the gold ions were reduced using the combination ST and SC (Fig. 4b). We have observed that there is no critical change in the size of AuNPs compared to the ST alone. However, the stability change was found to be more significant for colloidal AuNPs which were synthesized using a combination of ST and SC, their zeta potential value was relatively higher (40.2 mV), compared to the value of the particles obtained with ST alone (= 28.2 mV). This suggests that possibly the SC ions bind to the nanoparticles surface and act as stabilizing agent.

Characterization of supported AuNPs

The Au catalyst supported on different oxide carriers are first analyzed with XRF and then with the ICP method. XRF and ICP results (Table 1) showed that the loading of AuNPs on CaO, TiO_2 and Al_2O_3 is in line with the nominal content of Au (1 wt.%). The data presented in Table 1 shows the results of the comparison between XRF and ICP measurements. It can be seen from the Table that the results compare rather well. In general, XRF results of Au loading showed somewhat higher values compared to ICP results. Of course, there are small differences in the metal contents but these are all within the error margins of both the techniques.

BET surface areas and pore volumes of different pure supports and gold catalysts supported on different metal oxides are illustrated in Table 2. The surface areas and pore volumes are found to change significantly and strongly depend on the nature of support materials applied. Among all, Au/Al_2O_3 displayed the highest surface area while Au/CaO showed the lowest. As expected, the surface areas of the most of the supports were decreased to a certain extent upon the impregnation of the AuNPs. Nevertheless, both TiO_2 and Al_2O_3 supported catalysts did not show a noticeable effect on such decrease in the values of BET surface areas compared to their corresponding parent supports. These results indicate that the AuNPs are highly dispersed on the support probably without any sintering effect. Such good dispersion is also confirmed by XRD and TEM.

The XRD patterns of the fresh Au catalysts are depicted in Figure 5. Among all, the studied catalysts, Al_2O_3 supported Au catalyst is found to be X-ray amorphous, which is in agreement with the BET surface area data (261 m^2/g) (Fig. 5(a)). However, the XRD patterns of the fresh Au/TiO_2 sample also showed no reflections due to crystalline Au, indicating X-ray amorphous nature probably due to its crystallite size less than 5 nm (Fig. 5(b)). This observation lent good support to the observations made from TEM that confirmed the size of Au to be less than 3 nm. In addition, the sample reveals XRD reflections that corresponding to TiO_2 (anatase). In contrast, the XRD results of the CaO supported Au catalysts exhibited the crystalline gold metal phase in addition to intense reflections that corresponding to CaO (Fig. 5 (a)).

TEM images of gold catalysts supported on different metal oxide carriers are shown in Figure 6. At the first glance, it is obvious that the resulting Au particles show almost spherical shape with well dispersed state on the supports. It is also evident that the nature of support has shown a considerable influence on the Au particle size and their distribution. In order to check clearly such effect on the size of gold particles, the particle size distribution the TEM images are given in Figure 6 (insert Fig.). It should be noted that the size distribution was calculated by measuring more than a hundred individual gold particles using ImageJ software on digitized micrographs. Au diameter was calculated using the following formulae: $d_{Au} = n_i\, d_i\, / n_i$, where n_i is the number of Au particles of diameter d_i. These results indicate that among all catalysts, reducible carrier (TiO_2) found to give particles size with a narrow size distribution in the range from 0.6-4 nm. However, in case of using irreducible support (CaO and Al_2O_3), there is a considerable increase in the size of Au particles, which varies in the range from 1 to 6 nm. Interestingly, the morphology of the Au particles did not alter to a considerable extent in every case irrespective of the nature of support used. In other words, CaO support exhibits the biggest particles while TiO_2 support showed the smallest AuNPs.

Catalytic test

Effect of support on the catalytic performance of AuNPs in the solvent-free oxidation of BA using oxygen as an oxidant are portrayed in Figure 7. At first, blank tests without catalyst were carried out and no notable conversion of benzyl alcohol was observed (X-BA = 2.8 %). From this observation, it is clear that the catalytic performance of Au catalysts depends on the nature of the support applied. The catalytic activity is found to change in a similar way as that of Au particle size and obeys the following order: TiO_2 > Al_2O_3 > CaO (Fig. 7). It should be noted that the BAI is the major (target) product of the reaction. However, some by-products such as benzyl benzoate, benzoic acid and acetal were also observed in smaller amounts. The formation of the benzoic acid as a by-product is due to the over-oxidation of target product, benzaldehyde, while the formation of benzyl benzoate is expected from the esterification reaction of the benzoic acid and benzyl alcohol. It is evident from Fig. 7 that among all catalysts, the titania supported AuNPs are highly active (X-BA = 81%) and selective (S-BAI = 95%) in the oxidation of BA. The Au/Al_2O_3 catalyst showed relatively similar selectivity compared to Au/TiO_2 catalyst, but the conversion of BA is found to be three time less, which is more likely due to the presence of bigger AuNPs in this catalyst. Among the three supports, CaO displays relatively poor performance with low conversion of BA and low selectivity of BAI.
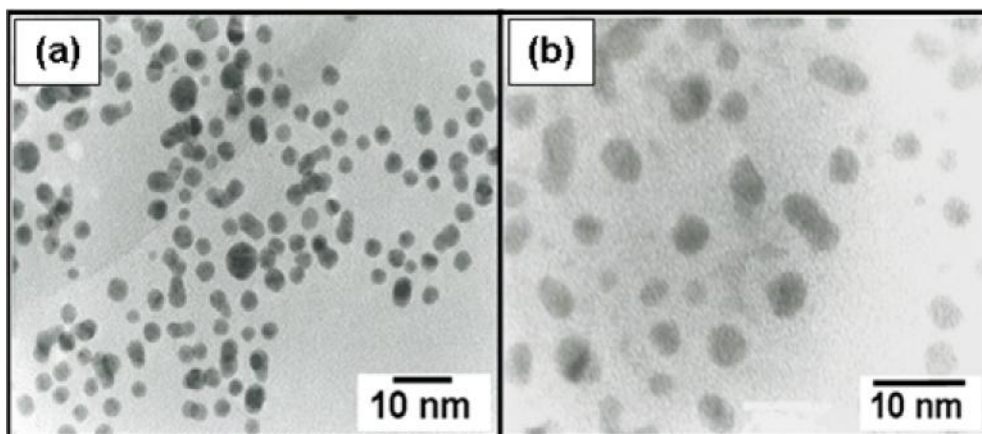
Fig. 4 TEM images of colloidal AuNPs prepared using a combination of **(a)** TA + SC and **(b)** ST + SC.

Table 1: XRF and ICP-OES results for Au catalysts supported on different metal oxides

Catalyst	Catalyst composition by XRF			Catalyst composition by ICP		
	Au	Support	Na^+, Cl^+	Au	Support	Na^+, Cl^+
Au/CaO	1.0	95.8	0.3	0.8	97.8	0.6
Au/TiO$_2$	1.1	95.8	0.1	0.9	98.8	0.1
Au/Al$_2$O$_3$	1.1	92.7	0.1	0.8	98.7	0.2

Table 2: BET-SA and pore volumes of gold catalysts on various oxide supports.

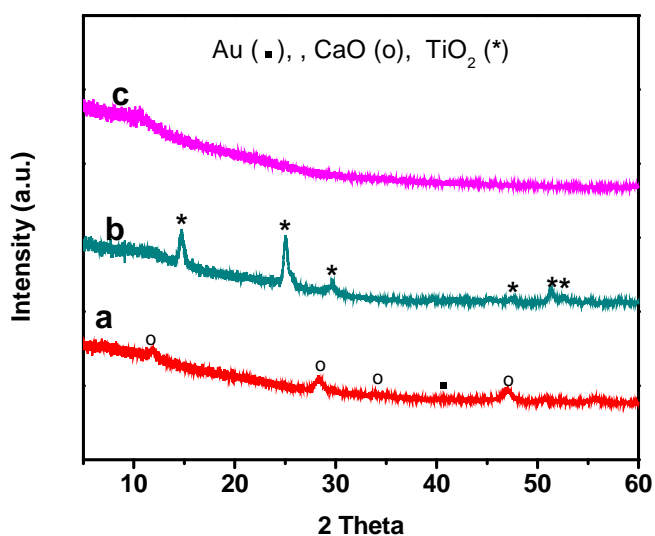| Entry	Catalyst	BET-SA (m^2/g)		Pore vol. of cat. (cm^3/g)
		Support	Catalyst	
1	Au/CaO	37	27	0.07
2	Au/TiO$_2$	47	43	0.12
3	Au/Al$_2$O$_3$	265	261	0.80

Fig. 5 XRD patterns of AuNPs supported on a: CaO, b: TiO$_2$, c: Al$_2$O$_3$.
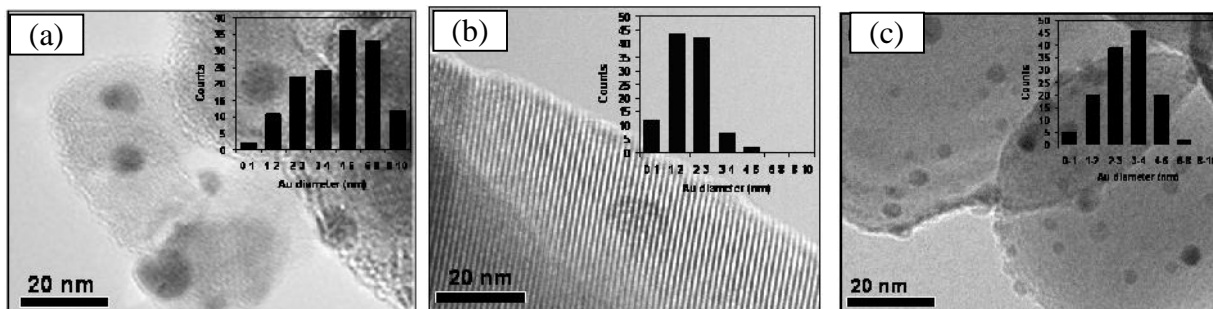
Fig. 6 TEM images of gold catalysts supported on a: CaO, b: TiO_2, and c: Al_2O_3. The distribution curves correspond to the TEM micrographs are presented in the insert.
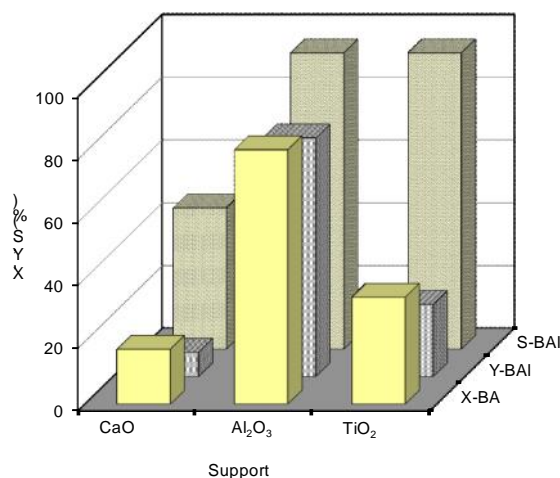

Fig. 7 Influence of metal oxide support on the oxidation of benzyl alcohol to benzaldehyde over 1% Au/S catalysts (S= CaO, TiO_2, Al_2O_3). (X-BA: conversion of benzyl alcohol; Y- BAl: yield of benzaldehyde and S-BAl: selectivity of benzaldehyde).

Conclusion

In summary, the formation of colloidal gold nanoparticles by the chemical reduction of tetrachloroauric acid [$HAuCl_4$] using various reducing agents was investigated in detail by different analytical methods such as UV-Vis, DLS and TEM. Results revealed that the morphology, average Au size, size distribution, and stability of such particles in colloidal mixture strongly depends on the synthesis conditions, nature of reductants and the type of support applied. Surprisingly, the combination of two reductants showed remarkable influence on the rate of reduction, size and reduction steps compared to the reduction using a single reductant. The smallest AuNPs of 3 nm average size could be successfully obtained using the combination of two reductants. In addition, preparation of gold colloids and their subsequent impregnation on different metal oxide was successful. Preliminary catalytic tests indicated that among all catalysts tested, gold supported on TiO_2 is found to be the best towards the oxidation of benzyl alcohol with 65% yield of benzaldehyde.

Conflict of Interest

The authors declare that there is no conflict of interests regarding the publication of this work.

32

References

Alshammari, A., A. Koeckritz, V. N. Kalevaru, A. Bagabas, and A. Martin. (2012). "Significant formation of adipic acid by direct oxidation of cyclohexane using supported nano-gold catalysts," Chem, Cat, Chem. 4(9): 1330–1336

Alvarez, M. M. J. T. Khoury, T. J. Schaaff, M. N. Shafigullin, I. Vezmar, and R. L. Whetten, (1997). "Optical absorption spectra of nanocrystal gold molecules," Journal of Physical Chemistry B, 101(19)P: 3706-3712

Bamwenda, G. R., S. Tsubota, T. Nakamura, and M. Haruta, (1997). "The influence of the preparation methods on the catalytic activity of platinum and gold supported on TiO_2 for CO oxidation," *Catalysis Letters*, 44(1-2): 83-87,

Berndt, H., A. Martin, I. Pitsch, U. Prüsse, and K. Vorlop, (2004). "Partial oxidation of polyvalent oxygen substituted compounds on nano-scale gold catalysts," Catalysis Today, 91-92: 191-194.

Bond, G. C. and D. T. Thompson, (1999). "Catalysis by gold," Catalysis Reviews - Science and Engineering, 41(3-4): 319-388

Bonet, F. and C. Guéry, D. Guyomard, R. H. Urbina, K. and Tékaia-Elhsissen, (1999). "Electrochemical reduction of noble metal compounds in ethylene glycol," International Journal of Inorganic Materials, 1(1): 47-51

Brust, M., M. Walker, D. Bethell, D. J. Schiffrin and R. Whyman, (1994). "Synthesis of thiol-derivatised gold nanoparticles in a two-phase Liquid–Liquid system" Journal of the Chemical Society, Chemical Communications, (7): 801-802,

Cheng, S.-Fang and L.-Kwan Chau, (2003). "Colloidal gold-modified optical fiber for chemical and biochemical sensing," Analytical Chemistry, 75(1): 16-21

Gaffet, E., M. Tachikart, O. El Kedim, R. and Rahouadj, (1996). "Nanostructurral materials formation by mechanical alloying: morphologic analysis based on transmission and scanning electron microscopic observations," Materials Characterization, 36(4-5): 185-190,

Goodman, C. M., C. D. McCusker, T. Yilmaz, and C. M. Rotello, (2004). "Toxicity of gold nanoparticles functionalized with cationic and anionic side chains," Bioconjugate Chemistry, 15(4): 897-900

Haruta, M. (1997). "Size- and support-dependency in the catalysis of gold," Catalysis Today, 36(1): 153-166

Haruta, M. (2002). "Catalysis of gold nanoparticles deposited on metal oxides," Catalysis Technology. 6(3):102-115

Haruta, M. (2005). "Catalysis: Gold rush" Nature. 437(7062): 1098-1099

Haruta, M. and M. Date, (2001). "Advances in the catalysis of Au nanoparticles," Applied Catalysis A: General, 222(1-2): 427–437

Hashmi, A. S. and K. G. Hutchings, (2006). "Gold catalysis," Angewandte Chemie International Edition, 45(47): 7896-7936

Hashmi, A. S. K., and G. J. Hutchings, (2013). "Gold Catalysis – the journey continues," Catalysis Science & Technology. 3(11): 2861–2861

http://www.malvern.com/LabEng/industry/colloids/colloids_stability.html.

Jaramillo, T. F., S. H. Baeck, B. R. Cuenya and E. W. McFarland, (2003). "Catalytic activity of supported Au nanoparticles deposited from block copolymer micelles," Journal of the American Chemical Society. 125(24): 7148–7165,

Kim, T., K. Lee , M.-S. Gong , S.-W. Joo, (2005). "Control of gold nanoparticle aggregates by manipulation of interparticle interaction," Langmuir, 21(21): 9524-9528

Lee K., and S.A. Asher, (2000). "Photonic crystal chemical sensors ph and ionic strength," Journal of the American Chemical Society,122(39): 9534-9537

Li, Y. and M. A. El-Sayed, (2001). "The effect of stabilizers on the catalytic activity and stability of Pd colloidal nanoparticles in the suzuki reactions in aqueous solution," *Journal of Physical Chemistry B*, vol. 105, no. 37, pp. 8938-8943

Mafune, F. J. Kohno, Y. Takeda, T. Kondow, (2003). "Formation of gold nano networks and small gold nanoparticles by irradiation of intense pulsed laser onto gold nanoparticles" Journal of Physical Chemistry B, 107(46): 12589-12596

Mohr, C., H. Hofmeister, J. Radnik and P. Claus, (2003). "Identification of active sites in gold-catalyzed hydrogenation of acrolein," Journal of the American Chemical Society, 125(7): 1905–1911

Mühlpfordt, H., (1982). "The preparation of colloidal gold particles using tannic acid as an additional reducing agent," Expirentia, 38(9): 1127-1128

Okitsu, K, A. Yue, S. Tanabe, H. Matsumoto, and Y. Yobiko, (2001). "Formation of colloidal gold nanoparticles in an ultrasonic field: control of rate of gold (III) reduction and size of formed gold particles," Langmuir, 17(25): 7717-7720

Paciotti, G. F: L. Myer, D. Weinreich, D. Goia, N. Pavel, R. E. McLaughlin, and L. Tamarkin, (2007). "Colloidal gold: a novel nanoparticle vector for tumor directed drug delivery," Drug Delivery, 11(3): 169-183

Prasad,B. L., S. I. Stoeva, and C. M. Sorensen, V. Zaikovski and K. J. Klabunde, (2003). "Gold nanoparticles as catalysts for polymerization of alkylsilanes to siloxane nanowires, filaments, and tubes," Journal of the American Chemical Society. 125(35): 10488–10396

Premkumar, T., D. Kim, K. Lee, K. E. Geckeler, (2007). "A facile and efficient 'one-step' synthesis of gold nanoparticles with tunable size," Gold Bulliten, 40(4): 321-327

Tiwari, P. M., K. Vig, V. A. Dennis, and S. R. Singh, (2011). "Functionalized gold nanoparticles and their biomedical applications," Nanomaterials, 1: 31-63

Turkevich, J., P. Stevenson, and J. Hillier, (1995). "A study of the nucleation and growth processes in the synthesis of colloidal gold," Discussions of the Faraday Society, 1: 55-75

Wang, Y. and Y. Xia, (2004). "Bottom-up and top-down approaches to the synthesis of monodispersed spherical colloids of low melting-point metals," Nano Letters, 10(10): 2048-2050,